The Scintigraphic Appearance of Alzheimer's Disease: A Prospective Study Using Technetium-99m-HMPAO SPECT

B. Leonard Holman, Keith A. Johnson, Basem Gerada, Paulo A. Carvalho, and Andrew Satlin

Department of Radiology, Brigham and Women's Hospital; Department of Neurology, Massachusetts General Hospital; Department of Psychiatry, McLean Hospital; and Departments of Radiology, Neurology and Psychiatry, Harvard Medical School, Boston, Massachusetts

Editor's Note: Please turn to p. 313 for corresponding editorial.

Alzheimer's disease produces regional abnormalities in brain blood flow and metabolism that may result in recognizable scintigraphic patterns. We determined the predictive value of ^{99m}Tc-HMPAO SPECT for the presence of Alzheimer's disease based on a prospective study of 132 consecutive patients coming to our nuclear medicine clinical unit for evaluation of their memory loss or cognitive abnormalities. During clinical follow-up averaging 10.1 mo, a final diagnosis was established in 113 patients, 52 of which had Alzheimer's disease. The probability of Alzheimer's disease was determined for seven scintigraphic patterns. The probability was 19% that patients with memory loss and normal perfusion had Alzheimer's disease. For abnormal perfusion patterns, the probability of Alzheimer's disease was 82% with bilateral temporoparietal defects, 77% with bilateral temporoparietal defects with additional defects, 57% with unilateral temporoparietal defects, 43% with frontal defects only, 18% with other large defects and 0% with multiple small cortical defects. We conclude that for ^{99m}Tc-HMPAO SPECT the predictive value of bilateral temporoparietal defects for Alzheimer's disease is high, while the perfusion patterns of unilateral temporoparietal perfusion defects and frontal defects only, which occur in 20% of patients with Alzheimer's disease, are not predictive of that disease.

J Nucl Med 1992; 33:181–185

Regional alterations in cortical blood flow and metabolism have been observed in patients with Alzheimer's disease using a variety of techniques including the inert gas washout method (*1–4*), PET (*5–9*), and perfusion SPECT (*10–16*). The predominant finding of bilateral temporoparietal abnormalities in these patients suggests a possible diagnostic role for functional imaging in the evaluation of memory and cognitive abnormalities. Clinical studies comparing patients with Alzheimer's disease and normal control subjects (*4,16–19*) or patients with multi-infarct dementia (*12,13,20,21*) suggest a high diagnostic accuracy for SPECT. Sporadic reports, however, warn that the perfusion defects associated with Alzheimer's disease may be nonspecific and may be seen in other conditions as well (*22–24*). We have determined the predictive value of a variety of scintigraphic patterns including bilateral temporoparietal defects for the presence of Alzheimer's disease when ^{99m}Tc-HMPAO SPECT is performed in patients with memory loss or cognitive abnormalities.

METHODS

All 132 patients referred to the nuclear medicine clinic for ^{99m}Tc-HMPAO SPECT between May 1989 and October 1990 with the principal complaint of memory or cognitive impairment were initially entered into this study. Final diagnosis was determined during clinical follow-up averaging 10.1 mo (range: 4 to 21 mo) by neurologists experienced in the diagnosis of dementia. Diagnosis of probable Alzheimer's disease was based on National Institute of Neurological Disease and Stroke/Alzheimer's Disease and Related Disorders Association criteria (NINDS/ADRDA) (*25*); diagnosis of other central nervous system diseases was based on standard criteria (*26*). Other imaging techniques including CT and/or MR were obtained in all cases and the results were incorporated into the final diagnosis. Nineteen of the 132 patients were dropped from the study; five of them because they were lost to follow-up and 14 of them because they continued to be diagnostic dilemmas.

The patients were studied using an annular single crystal brain camera (ASPECT), a digital SPECT system with a single-crystal sodium iodide ring detector and three collimators designed to view the patients' head from three angles simultaneously (*27*). The ring is rotated concentrically to the detector for three-dimensional reconstruction over a 21.4 cm (diameter) by 10.7 cm (length) field of view. Each of the collimator sections has hexagonal hole openings of 1 mm, a length of 2.4 cm and a septal thickness of 0.18 mm. The measured system resolution in air using capillary line sources is 8.2 mm at the center and 7.3 mm at 9 cm from the center for ^{99m}Tc. The sensitivity in air is 7.5 cps/μCi for a point source at the center.

Received Jul. 3, 1991; revision accepted Sept. 9, 1991.
For reprints contact: B. Leonard Holman, MD, Chairman, Department of Radiology, Brigham and Women's Hospital, 75 Francis St., Boston, MA 02115.

All patients were injected with 20 mCi of ^{99m}Tc-HMPAO while supine in a dimly lit room with background computer fans serving as white noise. Imaging began 10 min after injection with an acquisition time of 30 min (15 sec per projection) in 120 projections with a 360-degree rotation of the collimators. Two pulse-height analyzer windows were employed, one set at 140 ± 14 keV and one set to acquire scatter information from 112 to 126 keV. The combined set of projections were then corrected by subtracting 90% of the scatter projections and filtered to remove the forward scatter component from the photopeak projections. The projections were smoothed using a Butterworth filter (cutoff = 1.05 cycles per cm; power factor = 10), and then backprojected using a ramp filter. The reconstructed slices were corrected for attenuation using an attenuation factor of 0.15 cpm and displayed on a 128 × 128 matrix (1.67 × 1.67 mm) as a set of 64 slices (1.67 mm slice thickness). Coronal and sagittal displays were also calculated from the data set.

A method for image interpretation using a quantitative color scale was adapted from our previous experience using ^{123}I-isopropyl iodoamphetamine and a single-head rotating gamma camera (*17*). Each data set was reconstructed and displayed on a color monitor in axial, coronal and sagittal planes. Five 1.67-mm slices were summed to provide approximately 14 images, each with a slice thickness approximately equivalent to the spatial resolution of the instrument (8.3 mm). The monitor display format had a 16 component color scale with white representing the maximum of reconstructed activity. The color display level was individually adjusted for each patient so that the central area of the cerebellum was white (greater than 90% of the maximum activity of the slice), thus normalizing the entire data set to the ^{99m}Tc-HMPAO activity in the cerebellum. Data sets were classified as abnormal based on the appearance of reconstructed cortical activity that was less than 60% of the maximum activity (absence of white, yellow or red in an area of cortex on two or more slices).

Images were interpreted immediately after each study by one reader (BLH) who used the color display described above and who was knowledgeable of the criteria for abnormality but who was without knowledge of the clinical or laboratory data. Images were interpreted by noting the location, extent and severity of the perfusion defects. For ease of data analysis and interpretation, the SPECT studies were subsequently classified into the following perfusion patterns shown in Figure 1:

A: Normal.
B: Bilateral posterior temporal and/or parietal cortex defects.
C: Bilateral posterior temporal and/or parietal cortex defects with additional defects.
D: Unilateral posterior temporal and/or parietal cortex defects with or without additional defects.
F: Frontal cortex defects only.
F: Other large (>7 cm) defects.
F: Multiple small (≤7 cm) cortical defects.

Because the analysis routine was derived from [^{123}I]IMP rotating gamma camera SPECT data, the method was pretested on 15 control subjects (mean age: 68 ± 8.7 (s.d.) yr) without history of cerebrovascular or neurological disease by history, physical examination, and psychometric testing. Technetium-99m-HMPAO SPECT images were normal without cortical defects in all 15 subjects.

Patients were categorized according to presence (AD+) or absence (AD−) of Alzheimer's disease. The probability of Alz-

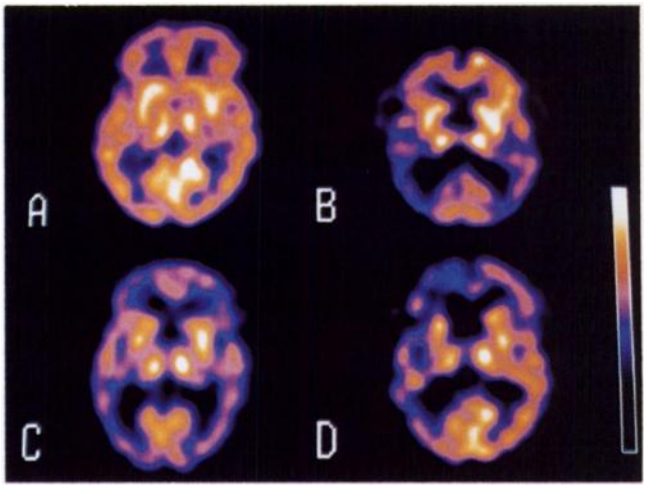

(A) Normal.
(B) Bilateral posterior temporal and/or parietal cortex defects.
(C) Bilateral posterior temporal and/or parietal cortex defects with additional defects.
(D) Unilateral posterior temporal and/or parietal. cortex defects with or without additional defects.
(F) Frontal cortex defects only.
(F) Other large (>one cm) defects.
(F) Multiple small (≤one cm) cortical defects.

FIGURE 1. Examples of ^{99m}Tc-HMPAO SPECT perfusion patterns. Pattern A: Normal perfusion. Pattern B: Bilateral posterior temporal and parietal defects. Pattern C: Bilateral posterior temporal and parietal defects with additional frontal defects. Pattern D: Left temporal, parietal and frontal cortex defects. Pattern E: Extensive bilateral frontal defects. Pattern F: Large defect involving the right lateral frontal and anterior temporal lobes. Pattern G: Multiple small cortical defects.

heimer (AD−) of Alzheimer's disease. The probability of Alzheimer's disease based on the scintigraphic perfusion pattern was determined with Bayes' theorem as described by McNeil (*28*) where $P(Q_i/AD+)$ is the probability of perfusion pattern Q_i in the presence of Alzheimer's disease and $P(Q_i/AD-)$ is the probability of perfusion pattern Q_i in patients without Alzheimer's disease.

RESULTS

We present our results as the frequency of disease occurrence for each of the scintigraphic patterns. When frequencies are categorized by final diagnosis, they represent the probability of disease for that scintigraphy pattern. Thus, $P(Q_B/AD+)$ is the probability that patients with bilateral posterior temporal and/or parietal perfusion defects (pattern B) have Alzheimer's disease and it is reported as a percentage of all patients with that perfusion pattern.

Patient Population

Fifty-two patients in this study had Alzheimer's disease. The final diagnosis in the other 61 patients was as follows: vascular dementia (11 patients), Parkinson's disease with

dementia (11 patients), HIV dementia (14 patients), Pick's disease (2 patients), epilepsy (3 patients), progressive supranuclear palsy (4 patients), depression (3 patients), head trauma (2 patients), systemic lupus erythematosus (2 patients), transient global amnesia (5 patients), primary progressive aphasia (1 patient) and no central nervous system disease (3 patients).

Frequency of Perfusion Patterns

Of the 113 patients in this study, 21 (18.6%) had normal and 92 (81.4%) had abnormal ^{99m}Tc-HMPAO SPECT studies. Pattern B (bilateral temporoparietal defects) was seen in 17 patients (15.0%), pattern C (bilateral temporoparietal defects and other defects) in 26 patients (23.0%), pattern D (unilateral temporoparietal defects with or without other defects) in 14 patients (12.4%), pattern E (frontal defects only) in 7 patients (6.2%), pattern F (other large defects) in 17 patients (15.0%), and pattern G (small cortical defects) in 11 patients (9.7%). Patterns B and C were asymmetrical in 38/43 (88.3%) patients with the left side worse than the right in 29 patients (67.4%).

Among the Alzheimer's disease patients, perfusion was normal in four patients (7.7%). Other patterns in the Alzheimer's disease patients were observed with the following frequency: pattern B in 14 patients (26.9%), pattern C in 20 patients (38.5%), pattern D in 8 patients (15.4%), pattern E in 3 patients (5.8%), and pattern F in 3 patients (5.8%) with Alzheimer's disease. Pattern F was not found in any patient with Alzheimer's disease.

Probability of Disease Based on the Perfusion Pattern

The probability of Alzheimer's disease ($P(Q_i/AD+)$) was 19% for normal perfusion, 82% for pattern B (bilateral temporoparietal defects), 77% for pattern C (bilateral temporoparietal and other defects), 57% for pattern D (unilateral temporoparietal defects), 42% for pattern E (frontal defects only), 18% for pattern F (other large defects) and 0% for pattern G (multiple small defects) (Table 1). All three patients with pattern B and without Alzheimer's disease had Parkinson's disease with dementia ($P(Q_B/PDD+) = 18\%$) (Table 2). The six patients with pattern C and without Alzheimer's disease had Parkinson's disease with dementia (3 patients) ($P(Q_C/PDD+) = 12\%$) and vascular dementia (3 patients) ($P(Q_C/VD+) = 12\%$). The six patients with pattern D and without Alzheimer's disease had Parkinson's disease with dementia (2 patients) ($P(Q_D/PDD+) = 14\%$), vascular dementia (3 patients) ($P(Q_D/VD+) = 21\%$), and primary progressive aphasia (1 patient) ($P(Q_D/PPA+) = 7\%$). The four patients with pattern E and without Alzheimer's disease had progressive supranuclear palsy (3 patients) ($P(Q_E/PSP+) = 43\%$) and SLE (1 patient) ($P(Q_E/SLE+) = 6\%$). All patients with pattern G (small cortical defects) had HIV dementia.

TABLE 1
Probability of Disease by Scintigraphic Pattern

Perfusion pattern	Probability of Alzheimer's disease	Probability of other diseases
A (normal)	19%	81% (including NL)
B (bilateral T/P)	82%	18% (18% PDD)
C (bilateral T/P + other)	77%	23% (12% PDD) (12% VD)
D (unilateral T/P)	57%	43% (22% VD) (14% PDD) (7% PPA)
E (frontal)	42%	58% (43% PSP) (15% HIV)
F (other)	18%	82% (many diseases)
G (multiple small)	0	100% (HIV)

NL = normal; PDD = Parkinson's disease with dementia; VD = vascular dementia; PPA = primary progressive aphasia; HIV = HIV dementia; and PSP = progressive supranuclear palsy.

TABLE 2
Distribution of Disease by Scintigraphic Pattern

SPECT pattern	Total patients per pattern	Final diagnosis												
		AD	PDD	VD	PSP	PD	HIV	TGA	Trauma	SLE	PPA	EP	DP	NL
A	21	4	2	3	0	0	2	1	0	1	0	2	3	3
B	17	14	3	0	0	0	0	0	0	0	0	0	0	0
C	26	20	3	3	0	0	0	0	0	0	0	0	0	0
D	14	8	2	3	0	0	0	0	0	0	1	0	0	0
E	7	3	0	0	3	0	0	0	0	1	0	0	0	0
F	17	3	1	2	1	2	1	4	2	0	0	1	0	0
G	11	0	0	0	0	0	11	0	0	0	0	0	0	0
Total patients per diagnosis	113	52	11	11	4	2	14	5	2	2	1	3	3	3

AD = Alzheimer's disease; PDD = Parkinson's disease dementia; VD = vascular dementia; PSP = progressive supranuclear palsy; PD = Pick's disease; HIV = HIV dementia; TGA = transient global amnesia; SLE = systemic lupus erthematosus; PPA = primary progressive aphasia; DP = depression; and NL = no CNS disease.

The three patients with pattern F (other defects) and Alzheimer's disease had perfusion defects involving the anterior temporal cortex (2 patients) and the anterior temporal and frontal cortex (1 patient). These defects were indistinguishable from the other 14 patients with this pattern except that the four patients with transient global amnesia all had unilateral medial temporal cortex perfusion defects. The remaining 10 patients with pattern F had Parkinson's disease with dementia (1 patient), Pick's disease (2 patients), HIV dementia (1 patient), progressive supranuclear palsy (1 patient), epilepsy (1 patient), trauma (2 patients), and vascular dementia (2 patients). Asymmetry was not helpful diagnostically in patients with patterns B and C since 22/34 (64.7%) of patients with Alzheimer's disease, 5/6 (83.3%) of patients with Parkinson's disease dementia, and 2/3 (66.7%) of patients with vascular dementia had more severe defects on the left.

DISCUSSION

While most studies have reported a high diagnostic accuracy for brain perfusion SPECT in Alzheimer's disease (*12–14,17,18,20,21*), its usefulness has been questioned because bilateral temporoparietal abnormalities are neither invariable (*14,29*) nor pathognomonic of the disease (*22–24,30*). Bilateral posterior defects have been described in patients with vascular dementia (*20*), Parkinson's disease (*22*), mitochondria encephalomyopathy (*23*), hypoglycemia (*24*) and carbon monoxide intoxication (*24*).

Most studies assessing the accuracy of SPECT in Alzheimer's disease have been retrospective with patient selection based on the diagnosis established at the time of the scintigraphic evaluation. Prospective, consecutive studies, while particularly difficult to perform because of the long follow-up necessary for accurate diagnosis, are more accurate guides to clinical practice (*21*). When a patient can be classified as probable Alzheimer's based on the National Institute of Neurologic Diseases and Stroke/Alzheimer's Disease and Related Disorders Association Criteria, the certainty of disease is over 90% in our experience. We therefore coupled our image analysis of consecutive cases with a clinical follow-up of sufficient duration to reduce the diagnostic uncertainty. As a result, the number of patients that could not be definitely classified was only ten percent of the total patient population. It is possible that Alzheimer's disease could have coexisted with other diseases in our study. However, confirmation of superimposed Alzheimer's disease would have required histopathologic evaluation.

We found a number of scintigraphic patterns in the patients coming to our nuclear medicine clinical unit for evaluation of memory and cognitive disorders. Those patterns with a high predictive value for Alzheimer's disease were bilateral temporoparietal defects with or without other defects (patterns B and C). The patterns of unilateral temporoparietal defects (pattern D) and frontal defects only (pattern E) were not predictive since they occurred in patients with Alzheimer's disease with similar frequencies as the disease occurred in the entire study population. The probability of Alzheimer's disease with normal perfusion (pattern A) or with perfusion defects outside of the temporoparietal cortex (pattern F) was low (19% and 18%, respectively) and follow-up perfusion SPECT will be necessary in these patients if their memory and cognitive skills continue to deteriorate.

Our results reflect the patient population of a tertiary care hospital with careful screening before referral to us. Consequently, almost half of the patients had Alzheimer's disease and only three were normal. We would expect somewhat different results in a community hospital setting with a higher number of normal subjects in the study population. The predictive value of a normal perfusion would be higher and the predictive patterns B and C might be somewhat lower.

We conclude that the scintigraphic pattern of Parkinson's disease with dementia cannot be distinguished from that of Alzheimer's disease by visual assessment alone. All of non-Alzheimer's patients with pattern B and half with pattern C had Parkinson's disease with dementia. While the Parkinson's disease patients had a variety of scintigraphic patterns, the most common involved the temporoparietal cortex. Our findings are consistent with other reports which describe decreased parietal cortex perfusion in Parkinson's disease patients (*24,30–32*). It is possible that some of these patients might have had Alzheimer's disease superimposed on their Parkinson's disease since these two common diseases may coexist.

Vascular dementia is due to a number of distinct underlying diseases (*33*). Binswanger's disease or subcortical atherosclerotic encephalopathy involves the microcirculation, is primarily a white matter disease, and is attributed to atherosclerosis of penetrating cerebral arteries. Multi-infarct dementia involves the large vessels and results from large cerebral infarcts. A third disease, a form of multi-infarct dementia but not usually involving large vessel occlusion, results from multiple small, deep, subcortical lacunar and pericapsular infarctions. Mixed forms of these three vascular diseases also occur. We lumped all patients with vascular dementia into one category because the various types cannot be accurately distinguished without histologic examination. Only 27% of patients classified as vascular dementia had bilateral involvement of the temporoparietal cortex. Consequently ^{99m}Tc-HMPAO SPECT appears reasonably accurate for distinguishing vascular dementia from Alzheimer's disease when patterns B and C are present.

In earlier studies using ^{123}I-isopropyl iodoamphetamine and single-head rotating gamma camera SPECT, we found unilateral posterior cortical defects in only 2% of our patients with Alzheimer's disease (*17*). Using ^{99m}Tc-HMPAO, we and others (*14*) have found unilateral posterior defects in 15%–20% of patients with Alzheimer's disease. Gemmell et al. have observed substantially more

perfusion defects with [^{123}I]IMP than with ^{99m}Tc-HMPAO SPECT (*34*), most likely due to the slower blood clearance of the latter agent. With higher resolution imaging systems, ^{99m}Tc-labeled ligands are preferred for studying cerebral perfusion because of the higher photon flux and, therefore, higher spatial resolution than with ^{123}I-labeled compounds. Other ^{99m}Tc agents, with more rapid blood clearance, such as ^{99m}Tc-ECD (*35*), may result in improved sensitivity for the detection of Alzheimer's disease and may lead to further refinement in the technique.

We conclude that ^{99m}Tc-HMPAO SPECT is useful in the diagnostic evaluation of patients with memory and cognitive abnormalities. The presence of bilateral posterior cortical defects indicate a high probability of Alzheimer's disease among patients referred for evaluation of dementia. Unilateral posterior defects and frontal defects are not predictive of Alzheimer's disease and these patients require further study. Patients with normal perfusion or with defects outside the posterior cortex have a lower probability of Alzheimer's disease, but, if the clinical suspicion is high or if memory and cognition is deteriorating, these patients should be restudied at a later date.

REFERENCES

1. Obrist WD, Chivian E, Cronqvist S, Ingvar DH. Regional cerebral blood flow in senile and presenile dementia. *Neurology* 1970;20:315–322.
2. Ingvar DH, Risberg J, Schwartz MS. Evidence of subnormal function of association cortex in presenile dementia. *Neurology* 1975;25:964–974.
3. Bonte FJ, Ross ED, Chehabi HH, Devous MD. SPECT study of regional cerebral blood flow in Alzheimer's disease. *J Comput Assist Tomogr* 1986;10:579–583.
4. Prohovnik I, Mayeux R, Sackeim HA, Smith G, Stern Y, Alderson PO. Cerebral perfusion as a diagnostic marker of early Alzheimer's disease. *Neurology* 1988;38:931–937.
5. Frackowiak RSJ, Pozzilli C, Legg NJ, et al. Regional cerebral oxygen supply and utilization in dementia. A clinical and physiological study with oxygen-15 and positron tomography. *Brain* 1981;104:753–78.
6. Friedland RP, Budinger TF, Ganz E, et al. Regional cerebral metabolic alterations in dementia of the Alzheimer type: positron emission tomography with [^{18}F]fluorodeoxyglucose. *J Comp Assist Tomogr* 1983;7:590–598.
7. Foster NL, Chase TN, Fedio P, Patronas NJ, Brooks RA, DiChiro G. Alzheimer's disease: focal cortical changes shown by positron emission tomography. *Neurology* 1983;33:961–965.
8. Friedland RP, Budinger TF, Brant-Zawadzki M, Jagust WJ. The diagnosis of Alzheimer-type dementia: a preliminary comparison of positron emission tomography and proton magnetic resonance. *JAMA* 1984;252:2750–2752.
9. Cutler NR, Haxby JV, Duara R, et al. Clinical history, brain metabolism, and neuropsychological function in Alzheimer's disease. *Ann Neurol* 1985;18:298–309.
10. Cohen MB, Graham LS, Lake R, et al. Diagnosis of Alzheimer's disease and multiple infarct dementia by tomographic imaging of iodine-123-IMP. *J Nucl Med* 1986;27:769–774.
11. Sharp P, Gemmell H, Cherryman G, Besson J, Crawford J, Smith F. Application of iodine-123-labeled isopropylamphetamine imaging to the study of dementia. *J Nucl Med* 1986;27:761–768.
12. Smith FW, Gemmell HG, Sharp PF. The use of ^{99m}Tc-HM-PAO for the diagnosis of dementia. *Nucl Med Commun* 1987;8:525–533.
13. Jagust WJ, Budinger TF, Reed BR. The diagnosis of dementia with single photon emission computed tomography. *Arch Neurol* 1987;44:258–262.
14. Neary D, Snowden JS, Shields RA, et al. Single photon emission tomography using ^{99m}Tc-HM-PAO in the investigation of dementia. *J Neurol Neurosurg Psych* 1987;50:1101–1109.
15. Johnson KA, Holman BL, Mueller SP, et al. Single photon emission computed tomography in Alzheimer's disease: abnormal I-123-iofetamine uptake reflects dementia severity. *Arch Neurol* 1988;45:392–396.
16. Johnson KA, Mueller ST, Walshe TM, English RJ, Holman BL. Cerebral perfusion imaging in Alzheimer's disease: use of single photon emission computed tomography and iofetamine hydrochloride I-123. *Arch Neurol* 1987;44:165–168.
17. Johnson KA, Holman BL, Rosen TJ, Nagel JS, English RJ, Growdon JH. I-123-iofetamine single photon emission computed tomography is accurate in the diagnosis of Alzheimer's disease. *Arch Intern Med* 1990;150:752–756.
18. Perani D, DiPiero V, Vallar G, et al. Technetium-99m-HM-PAO-SPECT study of regional cerebral perfusion in early Alzheimer's disease. *J Nucl Med* 1988;29:1507–1514.
19. Hellman RS, Tifofsky RS, Collier BD, et al. Alzheimer disease: quantitative analysis of I-123-iodoamphetamine SPECT brain imaging. *Radiology* 1989;172:183–188.
20. Deutsch G, Tweedy JR. Cerebral blood flow in severity-matched Alzheimer and multi-infarct patients. *Neurology* 1987;37:431–438.
21. Launes J, Sulkava R, Erkinjuntti T, et al. Tc-99m HMPAO SPECT in suspected dementia. *Nucl Med Commun* 1991;12:757–765.
22. Cohen D, Krausz Y, Lossos A, Ben-David E, Atlan H. Brain SPECT imaging with Tc-99m HM-PAO in Creutzfeld-Jakob disease. *Clin Nucl Med* 1989;14:808–810.
23. Grunwald F, Zierz S, Broich K, Schumacher S, Bockisch A, Biersack HJ. HMPAO-SPECT imaging resembling Alzheimer-type dementia in mitochondrial encephalomyopathy with lactic acidosis and stroke-like episodes (MELAS). *J Nucl Med* 1990;31:1740–1742.
24. Kuwabara Y, Ichiya Y, Otsuka M, et al. Differential diagnosis of bilateral parietal abnormalities in I-123 IMP SPECT imaging. *Clin Nucl Med* 1990;893–899.
25. McKhann G, Drachman D, Folstein M, Katzman R, Price D, Stadlan EM. Clinical diagnosis of Alzheimer's disease: report of the NINCDS-ADRDA Work Group under the auspices of Department of Health and Human Services Task Force on Alzheimer's disease. *Neurology* 1984;34:939–944.
26. Adams RD, Victor M. *Principles of neurology*, fourth edition. New York: McGraw Hill; 1989.
27. Holman BL, Carvalho PA, Zimmerman RE, et al. Brain perfusion SPECT using an annular single crystal camera: initial clinical experience. *J Nucl Med* 1990;31:1456–1561.
28. McNeil BJ. A diagnostic strategy using ventilation-perfusion studies in patients suspect for pulmonary embolism. *J Nucl Med* 1976;17:613–616.
29. Derouesne C, Rancurel G, LePoncin Lafitte M, Rapin JR, Lassen NA. Variability of cerebral blood flow defects in Alzheimer's disease on I-123-iodo-isopropylamphetamine and single photon emission tomography. *Lancet* 1985;11:1282.
30. Hoffman JM, Hanson MW, Earl NL, Coleman RE. Beware the classic FDG-PET pattern of Alzheimer's disease [Abstract]. *J Nucl Med* 1990;31:740.
31. Pizzolato G, Dam M, Borsato N, et al. [^{99m}Tc]-HM-PAO SPECT in Parkinson's disease. *J Cereb Blood Flow Metab* 1988;8:S101–108.
32. Nagel JS, Ichise M, Holman BL. The scintigraphic evaluation of Huntington's disease and other movement disorders using single photon emission computed tomography perfusion brain scans. *Semin Nucl Med* 1991;21:11–23.
33. Buell U, Costa DC, Kirsch G, Moretti JL, Van Royen EA, Schober O. The investigation of dementia with single photon emission tomography. *Nucl Med Commun* 1990;11:823–841.
34. Gemmell HG, Sharp PF, Besson JAO, Ebmeier KP, Smith FW. A comparison of TC-99m HM-PAO and I-123 IMP cerebral SPECT images in Alzheimer's disease and multi-infarct dementia. *Eur J Nucl Med* 1988;14:463–466.
35. Holman BL, Hellman RS, Goldsmith SJ, et al. Biodistribution, dosimetry, and clinical evaluation of technetium-99m-ethyl cysteinate dimer in normal subjects and in patients with chronic cerebral infarction. *J Nucl Med* 1989;30:1018–1024.